RESEARCH

Inhibition of the FEN1-PBX1 axis elicits cellular senescence in breast cancer via the increased intracellular reactive oxygen species levels

Min Wu[1,2*†][iD], Benmeng Wu[1,2†], Xiaoshan Huang[1,2†], Zirui Wang[1,2], Miaolin Zhu[3], Yaqin Zhu[1,2], Lin Yu[1,2] and Jingjing Liu[1,2*]

Abstract

Background Cellular senescence is a state of irreversible cell growth arrest. As such, senescence induction is viewed as an efficacious countermeasure in cancer treatment. Flap endonuclease 1 (FEN1) has been reported to participate in tumor growth, metastasis and immunomodulation. However, the role of FEN1 in cellular senescence of breast cancer and its molecular mechanism remains unclear.

Methods In vitro assessments of breast cancer cell senescence and apoptosis were conducted using CCK-8 assay, cell cycle assay, senescence-associated β-galactosidase (SA-β-gal) staining, and cleaved caspase-3 staining. Western blot, dihydroethidium (DHE) staining, RNA-sequencing, quantitative real-time polymerase chain reaction (qRT-PCR), rescue experiments, and dual-luciferase reporter assay were performed to explore the potential target of FEN1. Co-Immunoprecipitation (Co-IP), Chromatin immunoprecipitation (ChIP)-qPCR assay, and immunostaining were used to evaluate the interaction between FEN1 and Pre-B-cell leukemia homeobox transcription factor 1 (PBX1). A xenograft mouse model was employed to validate the effect of FEN1 on breast cancer cell senescence and apoptosis.

Results Functional analysis demonstrated that FEN1 suppressed both senescence and apoptosis of breast cancer cells in vitro, while in vivo experiments demonstrated moderate therapeutic effects. Further studies indicated that FEN1 deficiency promoted the aforementioned effects by increasing intracellular reactive oxygen species (ROS) levels. RNA-sequencing and qRT-PCR assays revealed that FEN1 knockdown enhanced the expressions of several senescence-associated secretory phenotype (SASP) factors and resulted in decreased PBX1 level. The rescue experiments by PBX1 overexpression verified that PBX1 mediated the senescence and apoptosis of breast cancer cells induced by FEN1 inhibition. In detail, FEN1 downregulation inhibited the transcription activity of PBX1, which was partially restored by itself overexpression. Of note, FEN1 directly interacted with PBX1. Furthermore, immunostaining

---

†Min Wu, Benmeng Wu and Xiaoshan Huang have contributed equally to this work.

*Correspondence:
Min Wu
minwu@yzu.edu.cn
Jingjing Liu
jjliu0105@163.com

Full list of author information is available at the end of the article

illustrated the colocalization of FEN1 and PBX1 in breast cancer cells and tissues. In our local breast cancer cohort, a positive correlation was identified between the expression levels of FEN1 and PBX1.

Conclusions Knockdown of FEN1 facilitates breast cancer cell senescence through PBX1 down-regulation mediating increase in intracellular ROS levels. This study reveals FEN1 as a negative regulator of cellular senescence and provides support for pro-senescence cancer therapy. Given that FEN1 knockdown exhibited only moderate in vivo effects, these findings underscore the necessity of combining it with senolytic therapy to enhance therapeutic efficacy.

Keywords Cellular senescence, FEN1, PBX1, ROS, Breast cancer therapy

Introduction

Breast cancer is the most prevalent malignant tumor in women and the second greatest cause of cancer-related deaths in females [1]. Although treatments such as surgery, chemotherapy, radiotherapy, targeted therapy, and endocrine therapy have indeed reduced the mortality rate among breast cancer patients [2], the high recurrence rates, drug resistance, and significant heterogeneity within breast cancer [3] lead to inadequate therapeutic outcomes and poor prognosis. Therefore, it is critical to explore novel therapeutic approaches and targets for breast cancer.

Cell senescence represents a multi-dimensional and highly heterogeneous state, marked by stable cell cycle arrest, the accumulation of senescence-associated β-galactosidase (SA-β-gal), resistance to apoptosis, and the activation of the senescence-associated secretory phenotype (SASP) [4]. SASP factors, including chemokines, cytokines, growth factors and enzymes, either initiate or strengthen senescence-associated growth arrest through autocrine or paracrine signaling, thus preventing tumor progression [5]. In addition, the regulation of certain genes can elicit cancer cell senescence, which in turn leads to the inhibition of tumor growth, such as extracellular signal-regulated kinase 5 (ERK5), non-neuronal SNAP25-like protein homologue 1 (NIPSNAP1), and ribose-5-phosphate isomerase A (RPIA) [6–8]. Thus, senescence induction is viewed as an efficacious countermeasure in cancer treatment [9].

There are various functions of reactive oxygen species (ROS), some of them contradictory, in the occurrence and development of tumor. Aquaporin 8 (AQP8) promotes the proliferation of glioma cells by triggering the ROS/phosphatase and tensin homologue (PTEN)/serine/threonine protein kinase (AKT) signaling pathway [10]. In contrast, WW domain-containing oxidoreductase (WWOX) suppresses the proliferation and migration of bladder cancer cells by elevating the levels of ROS [11]. Over recent years, the correlation between ROS and tumor cell senescence has been extensively investigated. Significant increases in ROS have been shown to be essential for both triggering and maintaining cellular senescence [12]. NIPSNAP decreases the levels of ROS by promoting the interaction between sirtuin 3 (SIRT3) and

superoxide dismutase 2 (SOD2), thereby inhibiting the senescence of colorectal cancer cells [7]. Downregulation of RPIA promotes the senescence of lung cancer cells by activating the ROS/p21 signaling pathway [8]. Therefore, the induction of ROS-mediated cellular senescence is a promising approach to impede tumor progression.

Pre-B-cell leukemia homeobox transcription factor 1 (PBX1), first identified in 1990, is regarded as a pioneer factor in cancer for manipulating oncogenic behaviors [13]. Park et al. revealed an association between PBX1 and proliferation in breast cancer cells in a Notch3-dependent manner [14]. Studies have shown that silencing PBX1 results in breast cancer cell apoptosis [15]. Moreover, the interaction between PBX1 and its transcription target, S100A10, regulates matrix metalloproteinase activity and the expression levels of stem cell-related genes, thereby promoting breast cancer invasion and enhancing metastasis ability [16]. Previous research demonstrated that increased PBX1 expression correlates with poor outcomes in breast cancer patients [17]. Consequently, PBX1 is a potential target, as well as a promising prognostic biomarker in breast cancer.

Flap endonuclease 1 (FEN1), a structure-specific nuclease, features prominently in numerous DNA metabolic pathways [18]. It has been demonstrated that FEN1 is significantly upregulated in several types of cancer, including non-small-cell lung cancer, breast and ovarian cancer [19, 20]. Sustained studies examining the role of FEN1 have focused on its impact on tumor growth and metastasis. For instance, FEN1 promotes breast cancer cell growth through the formation of the FEN1/proliferating cell nuclear antigen (PCNA) /DNA methyltransferases 3a (DNMT3a) complex [21]. In addition, FEN 1 enhances the migration/ invasion and epithelial-mesenchymal transition (EMT) process of hepatocellular carcinoma cells by facilitating USP7/MDM2-mediated P53 inactivation [22] and regulates the EMT of cholangiocarcinoma cells through the Wnt/β-catenin signaling pathway [23]. Our research showed that FEN1 mediated activation of STAT3 and facilitated proliferation and metastasis in breast cancer [24]. Moreover, the effects of FEN1 in immunomodulation have gradually come to light as functional study has increased. Down-regulation of FEN1 inhibits oral squamous cell carcinoma growth by

Wu *et al. Journal of Translational Medicine*   (2025) 23:248

Page 3 of 20

affecting immunosuppressive phenotypes via IFN-γ/JAK/STAT-1 [25]. Combination of downregulating FEN1 and PD-1 blockade enhances antitumor activity of CD8 + T cells against head and neck squamous cell carcinoma (HNSCC) cells in vitro [26]. A recent bioinformatics analysis shows that FEN1 is one of the senescence-related genes in gastric cancer [27]. Currently, there is a lack of studies on the regulatory role of FEN1 in cell senescence. Our investigation yielded compelling evidence, from both in vitro and in vivo experiments, that the downregulation of FEN1 elevates the intracellular ROS levels, which in turn accelerates the senescence of breast cancer cells. Importantly, we have identified that PBX1 as a target of FEN1 mediates the aforementioned effects of breast cancer cells induced by FEN1 inhibition. This study revealed that FEN1 is a negative regulator of cellular senescence and provided support for cellular senescence induction in cancer therapy.

Materials and methods

Cell culture and stable cell lines
The culture of human breast cancer cell lines (MDA-MB-231 and MCF-7) and the construction of stable cell lines were as described previously [24].

Bioinformatic analysis
FEN1 related genes were functionalized by Kyoto Encyclopedia of Genes and Genomes (KEGG) pathway analysis (https://www.linkedomics.org/admin.php). Steps are as follows: Cancer cohort: Breast invasive carcinoma → Search dataset: RNAseq → Search dataset attribute: FEN1 → Target dataset: RNAseq → Statistical method: Pearson Correlation test → Submit Query → Enrichment Analysis: KEGG Pathway. PBX1 expression in pan-cancer was acquired from Tumor Immune Estimation Resource, version 2 (TIMER2.0) database (http://timer.cistrome.org/). PBX1 expression in both normal and breast cancer tissues was acquired from Gene Expression Profiling Interactive Analysis, version 2 (GEPIA2) database (http://gepia2.cancer-pku.cn). The effect of PBX 1 expression on the prognosis of breast cancer patients was acquired from Kaplan-Meier plotter (http://kmplot.com/analysis/). The correlation between FEN1 and KIF15 at the mRNA level was obtained according to the ChiPBase v3.0 (https://rnasysu.com/chipbase3/index.php).

Breast cancer specimens
Breast cancer tumors and matched adjacent normal tissues were collected from patients at Jiangsu Cancer Hospital (Nanjing, Jiangsu, China) between June 2022 and October 2022. Exclusion criteria were: (a) male patients; (b) incomplete medical record; (c) history of other primary or secondary tumors. Supplementary Table 1 summarized the clinical information of 50 patients with breast carcinoma in this study. The TNM stage of all study patients was determined according to the criteria of the American Joint Committee on Cancer staging 8th edition [28]. The study followed the Declaration of Helsinki, got the informed consent signed by all patients and were approved from the Ethical Committee of Jiangsu Cancer Hospital.

Small interfering RNA (siRNA) and plasmid transfection
The siRNAs targeting NOX2 and FEN1 in this study were synthesized and purified by RiboBio (Guangzhou, China). The sequences of si-NOX2 and si-FEN1 are as follows: si-NOX2 (sense 5′-3′: UCAGGGUUCUUUAU UCUCUTT), si-FEN1 (sense 5′-3′: GACUGCCAGUG AAGCCAAATT). PBX1 plasmids were synthesized by Gene Create (Wuhan, China). Cells (6×10^5 or 3×10^5 / well) were seeded in 6 or 12-well plates. According to the manufacturer's instructions, siRNAs or plasmids were transfected into cells using Lipofectamine 3000 (Thermo Fisher, USA) in serum free medium, then cells were harvested after 24–48 h for later experiments.

RNA-sequencing analysis
The extraction and sequencing of RNA in the MDA-MB-231 line (sh-NC and sh-FEN1#1) were as described previously [24]. Differentially expressed genes were screened and identified mainly through the set|log2 (FoldChange)| and p values.

Quantitative real-time polymerase chain reaction (qRT-PCR)
Total RNA was extracted using Trizol Reagent (TransGen Biotech, Beijing, China). The purity and concentration of RNA were determined using NanoDrop 2000 spectrophotometer (Thermo Fisher Scientific, Waltham, ME, USA). Reverse-transcription was conducted using thermocycler (Thermo Fisher Scientific, Waltham, ME, USA) for synthesis of cDNA. The qRT-PCR was performed using QuantStudio3 (Thermo Fisher Scientific, Waltham, ME, USA). GAPDH was employed as the reference gene. Relative gene expression was calculated by the $2^{-\Delta\Delta CT}$ method. The relevant primer sequences (Tsingke, Beijing, China) are showed in Supplementary Table 2.

Western blot analysis
Cells were collected and lysed using the radioimmunoprecipitation buffer (Solarbio, Beijing, China) with addition of protease inhibitor cocktail (Roche, Switzerland). The protein concentration was measured by bicinchoninic acid (BCA) assay kit (Yeasen, Shanghai, China). Protein samples (20 μg/well) were separated by 8 ~ 12% SDS-PAGE gel and then shifted to polyvinylidene fluoride (PVDF) membranes (Sigma, Germany). Skim milk (5%) was used for blocking process. After that,

Wu *et al. Journal of Translational Medicine*   (2025) 23:248

Page 4 of 20

membranes were incubated with corresponding primary antibodies (Supplementary Table 3). Then membranes were incubated with secondary antibodies (Supplementary Table 3). Finally, the protein bands were visualized by using the Electrophoresis Gel Imaging Analysis System (Tanon, China) and the grey values were measured by Image J software to evaluate relative protein levels, and normalized to GAPDH.

Cell counting kit-8 (CCK-8) assay

Cell viability was evaluated using the commercial CCK-8 kit (Abbkine, Wuhan, China) per the manufacturer's protocol. Briefly, cells were seeded in 96-well plates (8×10^3 cells/ well) and treated with corresponding processes. Then the cells were incubated with the CCK-8 reaction solution for 2 h at 37 °C. After that, the optical density (OD) values were read at 450 nm to quantify the proliferation abilities of cells.

Cell cycle distribution

Cells (4×10^5/well) were trypsinized, washed, and fixed in 70% ice-cold ethanol. Subsequently, cells were washed and resuspended in RNase A for 30 min at 37 °C. Then, cells were labeled with propidium iodide at 4 °C for 30 min in the dark. Flow cytometry analysis was performed using BD FACSVerse™ Cell Analyzer (BD Biosciences, America) and cell cycle distribution was analyzed using FlowJo software.

SA-β-gal staining assay

For detecting cell senescence, SA-β-Gal Staining Kit (Solarbio, Beijing, China) was employed according to manufacturer's instructions. Firstly, cells (8×10^5/ well) were rinsed with PBS before adding 1mL of β-Gal staining fixative solution for 15 min at room temperature. Then cells were washed three times using PBS for 3 min and incubated with 1mL of β-Gal staining solution overnight at 37℃ without CO_2. The stained cells were detected with light microscope and the percentage of senescence cells was quantified using ImageJ in randomly selected fields ($n = 3$).

Measurement of cellular ROS levels by flow cytometry

To evaluate the ROS levels, dihydroethidium (DHE) staining was employed according to the manufacturer's instructions. Briefly, control and treated cells (4×10^5/ well) were washed twice with PBS, and then incubated with 10 μM DHE (KeyGEN, Nanjing, China) for 30 min at 37 °C in the dark. Then cells were washed three times to remove extracellular DHE and subjected to obtain fluorescence intensity via BD FACSVerse™ Cell Analyzer (BD Biosciences, America). Data were analyzed by FlowJo software. ROS levels were expressed as fold change over control.

Conditioned medium (CM) system

Breast cancer cells (MCF-7 and MDA-MB-231) with or without FEN1 knockdown were seeded in 6-well plate cultured in DMEM or DMEM-F12 medium containing 10% FBS for 24 h. Then, cells were washed twice with 1×PBS and then cultured in FBS-free DMEM or DMEM-F12 medium for 24 h. After that, medium was collected and centrifuged for 5 min at 1200 rpm, and then the supernatant was used to incubate with control cells (without FEN1 knockdown) for 24 h. Cultured cells were then tested for cell viability and cellular senescence.

Co-immunoprecipitation (Co-IP)

Cells (5×10^6) were lysed on ice in RIPA buffer containing 1% PMSF (Solarbio, Beijing, China). 10% of total cell lysates was used as Input group, and the remaining cell lysates were divided equally. Then the cell lysates were incubated with IgG (Proteintech, Wuhan, China) or primary antibodies (FEN1, PBX1) at 4 °C overnight on a rotator, followed by Protein A /G beads (Beyotime, Shanghai, China) for another 3 h of incubation. The supernatant was taken from the beads after centrifugation. The beads were washed three times using PBS, and then boiled with 5× Sample Loading Buffer (NCM Biotech, Suzhou, China) at 95 °C for 5 min. The co-precipitates were analyzed by western blot analysis.

Immunofluorescence

Cells (4×10^5/well) cultured on coverslips were washed with PBS, fixed with 4% paraformaldehyde for 20 min and permeabilized with 0.5% Triton X-100 for 10 min at room temperature. After blocking with 2% bovine serum albumin for 1 h at room temperature, the samples were incubated with primary antibodies (Supplementary Table 3) in 2% BSA overnight at 4 °C, followed by incubation with secondary antibodies (Supplementary Table 3) for 1 h at room temperature in the dark. Nuclei were stained with DAPI (Santa Cruz, CA, USA). Images were acquired by using fluorescence microscope or a laser confocal microscope with a 63x/ 1.40 oil objective lens with 340, 488 and 594 nm laser excitation (ZEISS, Germany). Results were analyzed by Image J software.

Dual-luciferase reporter assay

HEK293T cells (6×10^5/well) were seeded in 12-well plates and co-transfected with luciferase reporter plasmids containing KIF15 promoter (KIF15-Luc), TK-Renilla expression plasmids, along with indicated plasmids or siRNA by lipofectamine 3000 reagent. After 24 h, luciferase activity of each well was measured using the dual luciferase assay kit (TransGen Biotech, Beijing, China) following the manufacture's protocol. The Renilla activity was taken as a normalization of luciferase activity.

Chromatin immunoprecipitation (ChIP)-quantitative polymerase chain reaction (qPCR)

ChIP assays were conducted using the Sonication ChIP Kit (ABclonal Technology, Wuhan, China). In brief, HEK293T cells (1×10^7) were harvested and cross-linked with 1% formaldehyde for 15 min, and the reaction was terminated by addition of glycine. Then the samples were suspended in lysis buffer and sonicated on ice to generate DNA fragments with an average size of less than 1000 base pairs. After incubated with control IgG or Flag antibody overnight, cell lysates were incubated with protein A/G-agarose beads for another 3 h at 4 °C. Then beads were washed and eluted, and the cross links were reversed by incubation at 65 °C for 4 h. Finally, DNA was eluted and purified for qPCR analysis. The following ChIP-qPCR primers was used:

   KIF15-promoter-F, CGGATTCGCGACGATACAGA;
   KIF15-promoter-R, GAATTTGGCGCTTGGATCGG.

Immunohistochemistry (IHC)

Immunohistochemical staining was performed on formalin-fixed paraffin-embedded tissues. Tissue sections were heated at 60 °C for 1 h and dewaxed and rehydrated. Antigen recovery was performed and the sections were blocked with 3% hydrogen peroxide. Nonspecific staining was blocked with 10% goat serum. The sections were incubated with primary antibodies overnight at 4 °C, followed by incubation with horseradish peroxidase-conjugated secondary antibody for 30 min. DAB substrate was used for the chromogenic reaction and the sections were counterstained with hematoxylin. Primary antibodies used in IHC were listed in Supplementary Table 3. Tissue staining was evaluated using the IHC score as described previously [29].

Terminal deoxynucleotidyl transferase dUTP nick end labeling (TUNEL) assay

For detecting apoptosis situation in tumor samples, a TUNEL kit was utilized (Abbkine, Wuhan, China) following by the manufacturer's instructions. First, the paraffin-embedded sections were dewaxed and hydrated using standard procedures. After shaking the sections dry, the sections were incubated proteinase K working solution (Thermo Fisher, USA) for 15 min at 37 °C, and then treated with 50 µL of TdT labeling buffer by incubation for 1 h at 37 °C in a moist black box. Then the DAPI staining solution was added to the sections for staining for 10 min at room temperature in the dark. The sections were blocked with an anti-fluorescence quenching sealing agent. Finally, we obtained images by operating a fluorescence microscope.

Establishment of xenograft models

Four-week-old female BALB/c nude mice were purchased from the Animal Research Center of Yangzhou University (Yangzhou, China) and permitted to acclimatize for seven days. Stable FEN1 knockdown (sh-FEN1#1) or negative controls (sh-NC) MDA-MB-231 cells (5×10^6 cells/mouse, four/group) were subcutaneously inoculated into the right flanks of mice. The growth of tumor size (L, longest dimension; W, shortest dimension) was evaluated by the vernier caliper every five days, and tumor volumes were calculated using the formula ($V = L \times W \times W/2$). After six weeks, mice were euthanized and the tumors were then collected for additional research. The maximum diameter of the tumor masses measured is less than 15 mm. Tumor growth inhibition (TGI) is calculated using the formula: TGI (%) = [1-(Ti-T0)/ (Vi-V0)] ×100; Ti is the average tumor volume of a treatment group on a given day, T0 is the average tumor volume of the treatment group on day 0, Vi is the average tumor volume of the control group on the same day with Ti, and V0 is the average tumor volume of the group on day 0.

Statistical analysis

Data were presented as mean ± standard deviation (SD). The Student's t-test was used to compared the differences between two groups, and the one-way ANOVA analysis was conducted to compare multiple groups. Results were analyzed utilizing the SPSS 19.0 and GraphPad Prism 9 software. Statistical significance was set at $p < 0.05$.

Results

FEN1 impedes the senescence and apoptosis of breast cancer cells

Previous research has indicated that there is a high level of FEN1 expression in breast cancer [20]. In our study, FEN1 expression was detected by Western blot in breast cancer cell lines (BT-549, MCF-7, MDA-MB-231) and normal breast cell line (MCF-10 A). As the results indicated, the expression of FEN1 in these two cell lines (MCF-7 and MDA-MB-231) were higher compared to MCF-10 A or BT-549 (Fig. 1A). Based on the above, these two cell lines (MCF-7 and MDA-MB-231) were selected for our study.

To investigate the effect of FEN1 on the senescence of breast cancer cells, breast cancer cell lines with stable overexpression and knockdown of FEN1 were constructed.

The cells infected with lentivirus vectors were observed under the fluorescence microscope. The lentivirus infection efficiencies were over 90% (Fig. S1A-B). When the cells infected with lentivirus vectors became stable cell lines, FEN1 overexpression and knockdown were confirmed by Western blot [24]. Since senescent cells have typical feature, such as low proliferation and cell cycle
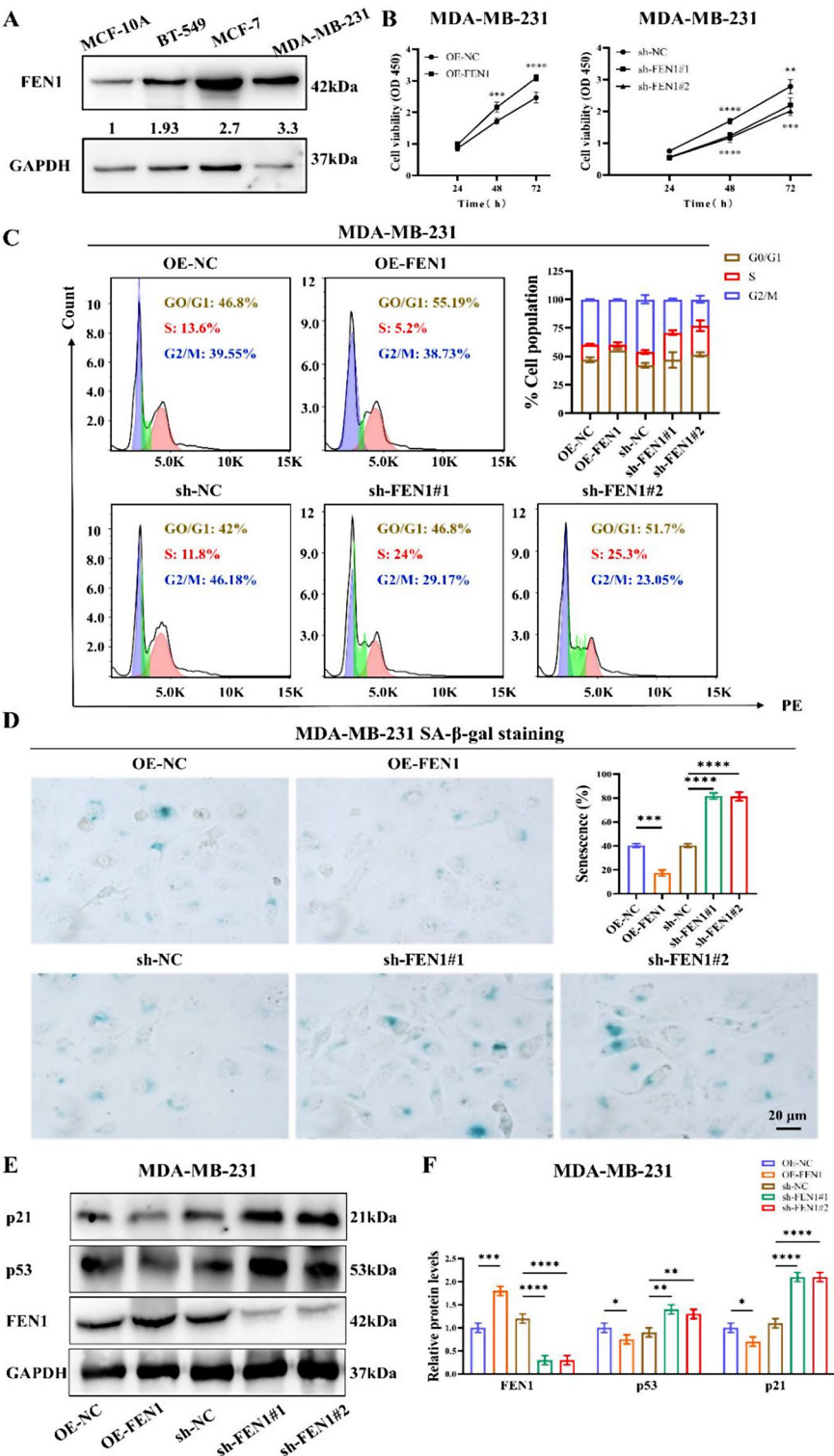
Fig. 1 FEN1 significantly represses cell senescence in MDA-MB-231 cells. **A** FEN1 expression was detected by Western blot in breast cancer cell lines and normal breast cell line. **B** CCK8 analysis of cell viability in FEN1-overexpression or knockdown cells. **C** Cell cycle distribution measured by flow cytometry in FEN1-overexpression or knockdown cells. **D** SA-β-gal staining analysis in FEN1-overexpression or knockdown cells. **E-F** Western blot analysis of FEN1, p53 and p21 in FEN1-overexpression or knockdown cells (**E**, representative blots; **F**, quantified results). Results are presented as mean ± SD from three independent experiments, * $p < 0.05$, ** $p < 0.01$, *** $p < 0.001$, **** $p < 0.0001$

arrest, CCK8 assay was performed to detect the effect of FEN1 on cell proliferation, and cell cycle distribution was determined by flow cytometry. The results illustrated that FEN1 facilitated breast cancer cell proliferation (Fig. 1B and Fig. S2 A), and low FEN1 expression increased the S phase ratio leading to cell cycle arrest, whereas high FEN1 expression resulted in a significant reduction in the proportion of S phase cells (Fig. 1C and Fig. S2 B). Furtherly, the level of SA-β-gal was measured, and the results showed that the percentage of SA-β-gal-positive cells were significantly increased in FEN1 knockdown cells, while FEN1 overexpression had the opposite effect (Fig. 1D and Fig. S2 C), indicating that FEN1 inhibited breast cancer cell senescence. Besides, the effect of FEN1 expression on apoptosis was also examined by cleaved caspase-3 immunostaining. The findings revealed that FEN1 overexpression suppressed the levels of cleaved caspase-3 when compared to the control group, whereas the reduction of FEN1 expression led to an increase in cleaved caspase-3 expression (Fig. S3 A-B). Moreover, we analyzed the expression levels of several senescence related molecules (the cell cycle arrest protein p21 and pivotal regulator of senescence p53) and apoptosis related markers (pro-apoptosis protein Bax and anti-apoptosis protein Bcl-2). In breast cancer cells with FEN1 overexpression, levels of p21, p53 and Bax were reduced, while Bcl-2 levels were increased. Conversely, breast cancer cells with FEN1 knockdown demonstrated increased levels of p21, p53 and Bax, while Bcl-2 levels decreased (Fig. 1E-F, Fig. S2 D, and Fig. S3 C-D). These findings indicate that FEN1 suppresses both senescence and apoptosis in breast cancer cells.

FEN1 deficiency promotes the senescence and apoptosis of breast cancer cells by increasing intracellular ROS levels

Elevated intracellular ROS levels is a significant factor contributing to cell senescence and apoptosis [30]. Does ROS mediate the cellular senescence and apoptosis induced by FEN1? Intracellular ROS was assessed with DHE staining and flow cytometry analysis. The results showed that an increase in FEN1 expression led to reduced intracellular ROS levels, whereas decreased FEN1 expression caused an increase (Fig. 2A and Fig. S4 A). This implies that FEN1 could potentially regulate senescence and apoptosis in breast cancer cells via ROS. Next, we pretreated breast cancer cells with the N-acetylcysteine (NAC, 10 mM), a specific ROS scavenger, for 30 min, after which the cells were cultured for an additional 24 h. Subsequently, we conducted ROS level detection and SA-β-gal staining. The data demonstrated that NAC pretreatment effectively attenuated ROS levels (Fig. 2B and Fig. S4 B) and the percentage of SA-β-gal-positive cells compared with control groups (Fig. 2C and Fig. S4 C). Consistent with expectations, NAC

treatment completely blocked the promoting effects of FEN1 knockdown on cellular senescence and apoptosis (Fig. 2D-E and Fig. S4 D-E). These findings indicate that a reduction in FEN1 expression elevates intracellular ROS levels, thereby promoting senescence and apoptosis of breast cancer cells. Mitochondria and NADPH oxidase serve as the principal sources of intracellular ROS [31]. NADPH oxidase 2 (NOX2) and NOX4 represent the two key types of NADPH oxidases [32]. Our study demonstrate that FEN1-mediated ROS are mainly derived from NOX2 (Fig. S 5).

PBX1 is identified as a potential target of FEN1

To uncover the mechanism of FEN1 regulating breast cancer cell senescence, MDA-MB-231 stable cell lines (sh-NC and sh-FEN1#1) underwent transcriptome sequencing analysis (Fig. 3A). The up-regulated genes in FEN1 down-regulated cells included several SASP factors (C-X-C motif chemokine ligand 1/2/8/10/11(CXCL1, CXCL2, CXCL8, CXCL10, CXCL11), C-X3-C Motif Chemokine Ligand 1(CX3CL1), C-C Motif Chemokine Ligand 5 (CCL5), Interleukin 6/18 (IL6/18), Interleukin-1 alpha (IL-1α), and Matrix metallopeptidase 1(MMP1)) closely related to cell senescence (Fig. 3B). The sequencing results indicated that FEN1 was involved in the senescence of breast cancer cells. Furthermore, the qRT-PCR analysis of common SASP factors revealed a substantial increase in the expressions of IL6, IL8, IL-1β, Tumor necrosis factor- alpha (TNF-α), and MMP1 in FEN1 down-regulated cells as compared to the control (Fig. 3C).

Recent studies suggest that SASP factors in cancer have both anti-tumor and pro-tumor effects [33]. To confirm the effect of SASP factors secreted by senescent cells, control cells were exposed to conditioned medium (CM) from cells with or without FEN1 knockdown. Upon incubation with CM from FEN1 knockdown cells, reduced cellular proliferation with a higher percentage staining for SA-β-gal was evident relative to the control CM-treated counterparts (Fig. S 6 A-C). The above results suggest that SASP factors secreted by FEN1-knockdown cells might inhibit cell proliferation and promote cell senescence. Certainly, NAC pretreatment mitigated the elevated SASP factor levels induced by FEN1 knockdown (Fig. 3E), further confirming the involvement of ROS in cell senescence elicited by FEN knockdown. Additionally, Kyoto Encyclopedia of Genes and Genomes (KEGG) enrichment analysis of genes significantly associated with FEN1 expression in breast cancer showed that related genes were enriched in cell senescence (Fig. 3D). These results underscore a profound association between FEN1 and the senescence of breast cancer cells.

Subsequently, we screened the top 20 genes significantly related to FEN1 and PBX1 was identified as one
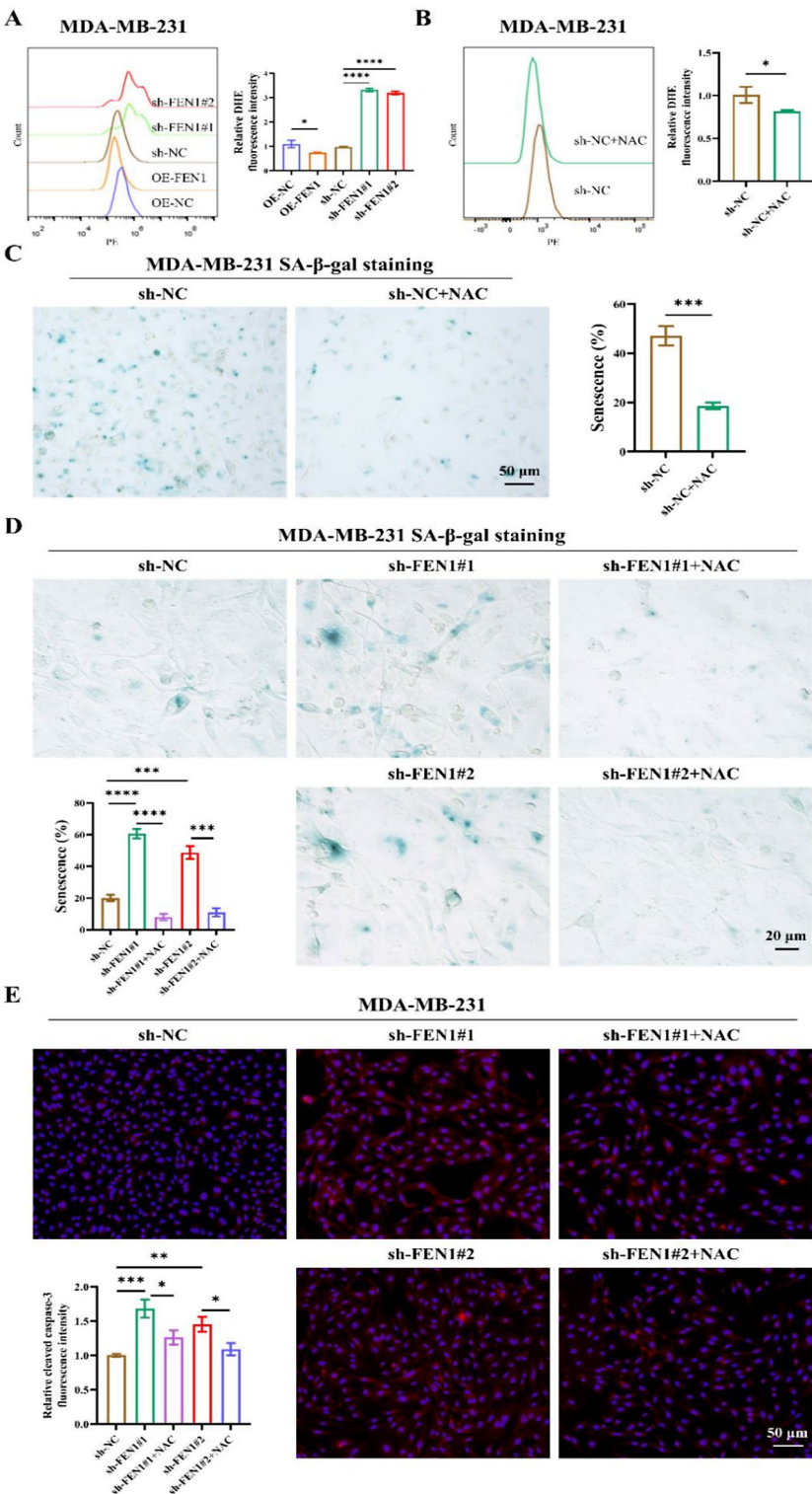
Fig. 2 FEN1 deficiency promotes cell senescence and apoptosis by increasing intracellular ROS levels in MDA-MB-231cells. **A** Intracellular ROS levels were detected with DHE staining by flow cytometry in FEN1-overexpression or knockdown cells. **B** Intracellular ROS levels in MDA-MB-231 cells pretreated with or without NAC (10 mM, 30 min). **C** SA-β-gal staining analysis in MDA-MB-231 cells pretreated with or without NAC (10 mM, 30 min). **D** SA-β-gal staining analysis in FEN1-knockdown cells pretreated with or without NAC (10 mM, 30 min). **E** Immunofluorescence staining analysis of cleaved caspase-3 in FEN1-knockdown cells pretreated with or without NAC (10 mM, 30 min). Results are presented as mean ± SD from three independent experiments, * $p < 0.05$, ** $p < 0.01$, *** $p < 0.001$, **** $p < 0.0001$
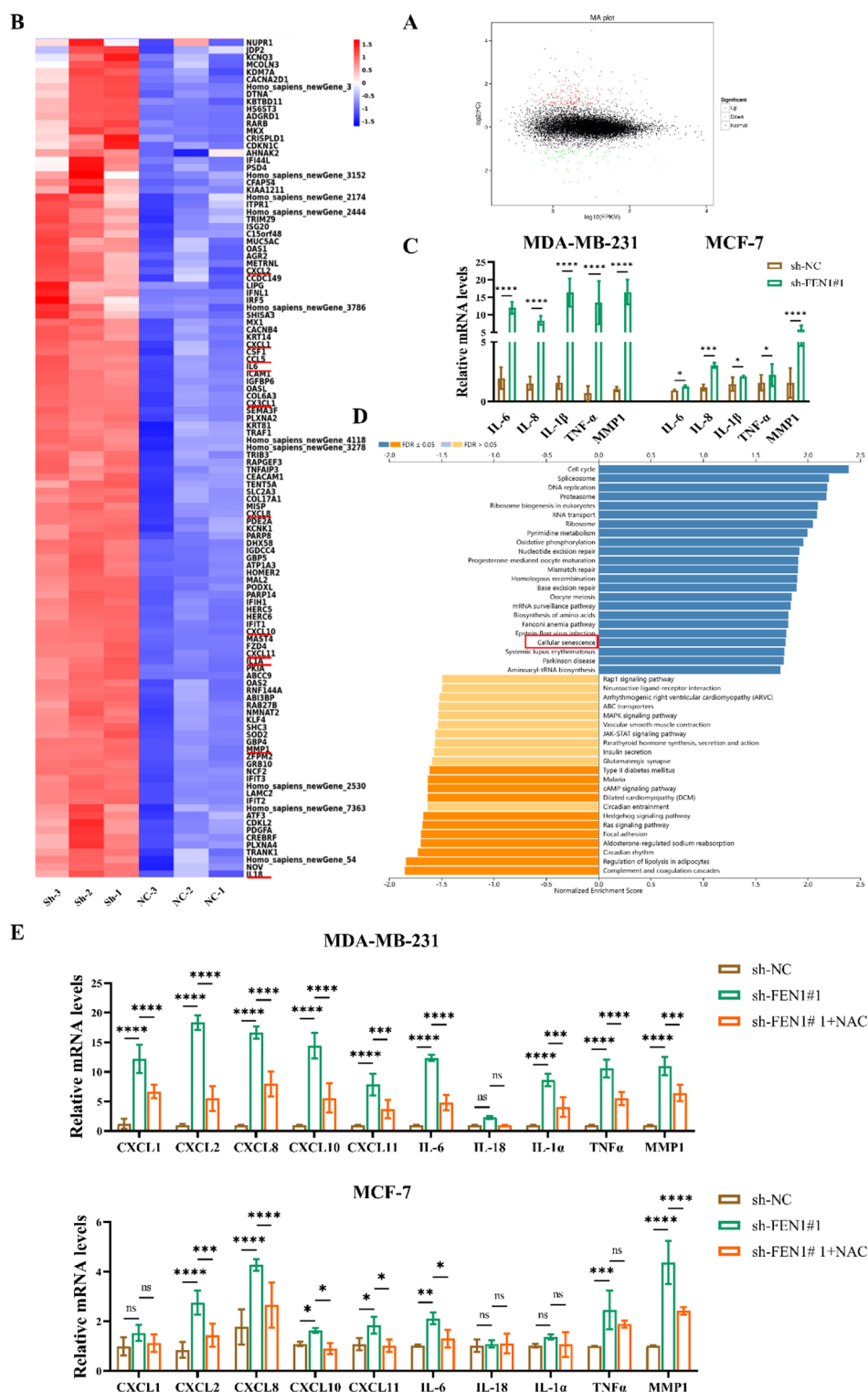
Fig. 3 FEN1 is involved in the senescence of breast cancer cells. **A** Volcano plot analysis in sh-FEN1#1 vs. sh-NC MDA-MB-231 cells. **B** Upregulated genes (including SASP factors) in sh-FEN1#1 MDA-MB-231 cells were shown in the heatmap. **C** qRT-PCR analysis revealed that the expressions of common SASP factors (IL6, IL8, IL-1β, TNF-α, and MMP1) were increased in FEN1 knockdown cells. **D** KEGG enrichment analysis indicated enrichment in cell senescence. **E** SASP factors were detected by qRT-PCR in breast cancer cells with or without FEN1-knockdown pretreated with or without NAC (10 mM, 30 min). Results are presented as mean ± SD from three independent experiments, ns: no significance, * $p < 0.05$, ** $p < 0.01$, *** $p < 0.001$, **** $p < 0.0001$

of the potential targets of FEN1 (Fig. 4A). PBX1 has been regarded as a novel master regulator in cancer [13]. Our bioinformatics analysis showed that PBX1 is highly expressed in breast cancer tissues, and its high expression is related to the poor prognosis of patients (Fig. S 7), further confirming that PBX1 is involved in breast cancer progression. To explore the role of PBX1 in breast cancer, breast cancer cells were transfected with the plasmids expressing PBX1 to achieve high levels of PBX1 expression in the cells (Fig. 4B-D). Concordantly, PBX1 overexpression suppressed the levels of intracellular ROS in breast cancer cells compared with the control (Fig. 4E-F). To examine whether PBX1 influences senescence and apoptosis in breast cancer cells via ROS, PBX1-overexpressing cells were treated with or without the ROS activator 2-methoxyestradiol (2-ME2). The results showed that 2-ME2 treatment restored the down-regulated ROS levels (Fig. 4E-F). As expected, overexpression of PBX1 suppressed both senescence and apoptosis in breast cancer cells when compared to control cells (Fig. 4G-J). Nevertheless, 2-ME2 partially or completely rescued the attenuated senescence and apoptosis caused by PBX1 overexpression (Fig. 4G-J). These findings suggest that PBX1 represses the senescence and apoptosis of breast cancer cells partially through the downregulation of ROS levels. This is also the first demonstration that PBX1 is involved in tumor cell senescence.

PBX1 mediates the senescence and apoptosis of breast cancer cells induced by FEN1 inhibition

To explore the relationship between FEN1 and PBX1, the effect of FEN1 knockdown on PBX1 expression was detected. The mRNA and protein levels of PBX1 were decreased after FEN1 knockdown (Fig. 5A-C). Hence, to examine whether FEN1 influences subsequent effects via PBX1, FEN1 knockdown cells were transfected with PBX1-expressing plasmids. The ectopic expression of PBX1 was verified in FEN1 down-regulated breast cancer cells transfected by PBX1-expressing plasmids (Fig. 5D-E), and the results showed that PBX1 overexpression mitigated the ROS levels increased by FEN1 down-regulation (Fig. 5F-G). Importantly, overexpression of PBX1 strongly counteracted cancer cell senescence and apoptosis exacerbated by downregulation of FEN1 (Fig. 5H-K). Thus, FEN1 downregulation elevated ROS levels via PBX1 downregulation, thereby accelerating breast cancer cell senescence and apoptosis.

FEN1 deficiency inhibits the transcription activity of PBX1 and FEN1 interacts with PBX1

PBX1 is known to be a transcription factor that promotes tumor progression by regulating the transcription of downstream target genes. According to the above results, downregulation of FEN1 mainly exerted its effect by down-regulating PBX1 expression. Does FEN1 also affect the transcription activity of PBX1? Kinesin family member 15 (KIF15) has been identified as a potential target gene of PBX1 [34]. In addition, downregulation of KIF15 contributes to tumor cell cycle arrest and increased intracellular ROS levels, thereby hindering tumor progression [35, 36]. We found that PBX1 overexpression significantly increased KIF15 mRNA level (Fig. 6A). To verify whether FEN1 affects the transcription activity of PBX1, the luciferase plasmid containing the KIF15 promoter region was constructed. The dual-luciferase reporter assay confirmed that PBX1 enhanced the transcription of KIF15 promoter (Fig. 6B). When FEN1-specific siRNA was introduced, the transcription level of KIF15 promoter decreased, but could be partially restored with PBX1 overexpression (Fig. 6B), showing that FEN1 downregulation decreased the transcription activity of PBX1. According to the ChiPBase v3.0 project, there exists a positive correlation between FEN1 and KIF15 at the mRNA level (Fig. 6C). Further investigations confirmed that FEN1 downregulation reduced both mRNA and protein levels of KIF15 (Fig. 6D-F), which were rescued by PBX1 overexpression (Fig. 6D-F), alongside alterations in p21 and p53 (Fig. 6E-F). These findings further support that FEN1 downregulation inhibits the transcription activity of PBX1.

Despite these findings, other mechanisms where FEN1 might impact PBX1's transcription activity, suggested by earlier studies on protein interactions with transcription factors [37, 38], should not be disregarded. The interaction between FEN1 and PBX1 in breast cancer cells (Fig. 7A), along with their colocalization in breast cancer cells (Fig. 7B) and tissues (Fig. 7C), were verified. To assess the impact of FEN1 knockdown on PBX1 expression by immunofluorescence staining, FEN1 small interfering RNA (si-FEN1) was employed to transfect breast cancer cells. The results revealed that the transfection with si-FEN1 decreased the mRNA and protein levels of both FEN1 and PBX1 in the cells (Fig. S 8 A-B). Immunostaining further confirmed that FEN1 knockdown lead to a decrease in PBX1 expression, resulting in a significant reduction in the colocalization of FEN1 and PBX1(Fig. 7D). In addition, we conducted ChIP-qPCR assays on HEK293T cells that ectopically expressed Flag-PBX1 or Flag-FEN1. The enrichment was significantly increased when FEN1 or PBX1 expression was upregulated, compared with control (Fig. 7E), showing that PBX1 and FEN1 were enriched in the same region of the KIF15 promoter. Together, there is interaction between FEN1 and PBX1, and the transcription activity of PBX1 is inhibited upon FEN1 downregulation.
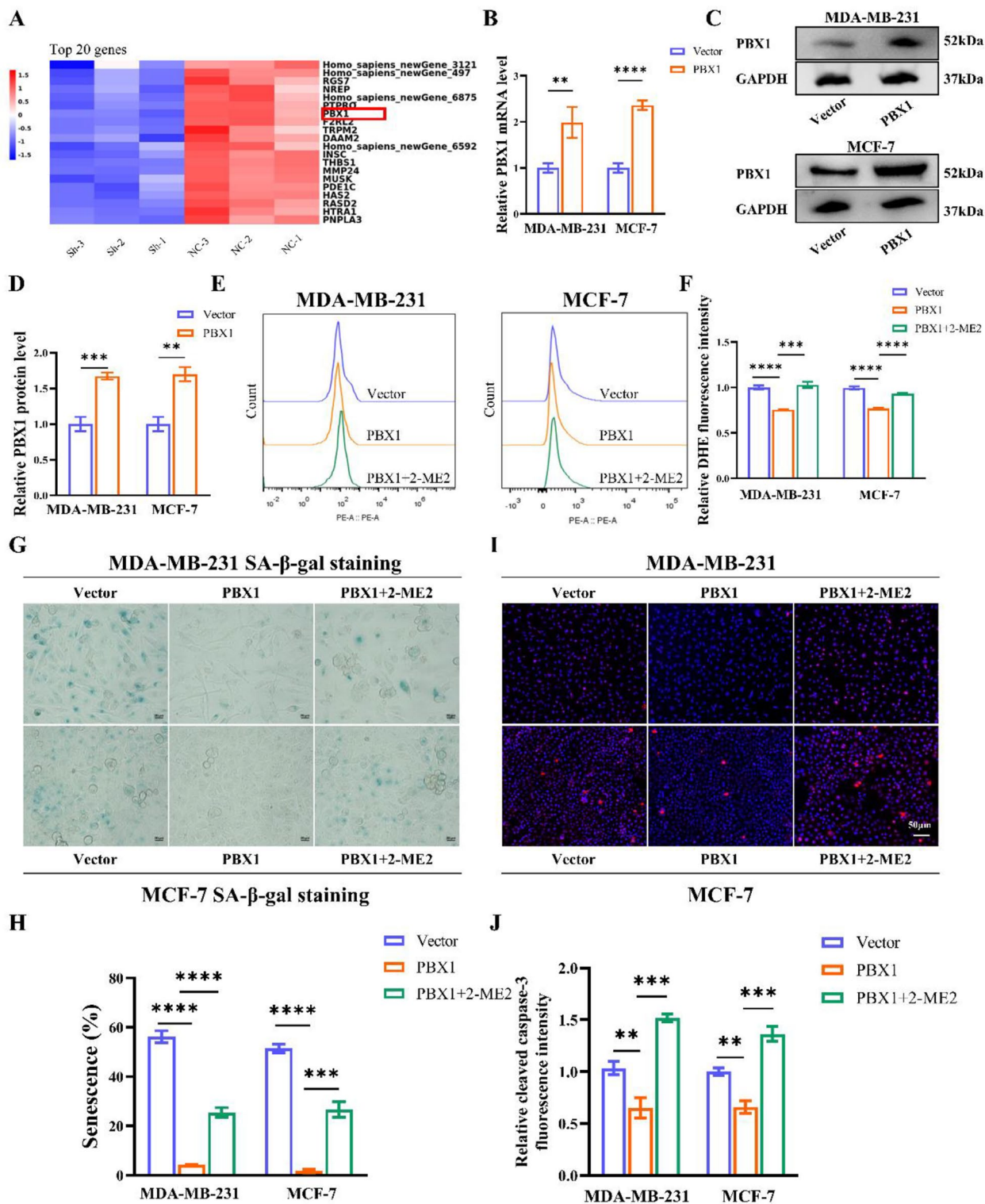
Fig. 4 PBX1 is identified as a potential target of FEN1. **A** The downregulated 20 genes in sh-FEN1#1 vs. sh-NC MDA-MB-231 cells were shown in the heat-map. In breast cancer cells transfected with the plasmid expressing PBX1(2.5 μg, 48 h), overexpression of PBX1 was confirmed by qRT-PCR (**B**) and Western blot (**C-D**). **E-F** Intracellular ROS levels, **G-H** positive rates of SA-β-gal staining, as well as **I-J** the expression of cleaved caspase-3 were decreased in breast cancer cells transfected with PBX1-expressing plasmids (1 μg, 48 h) but increased after cells treated with 2-ME2 (10 μM, 24 h). Results are presented as mean ± SD from three independent experiments, ** $p < 0.01$, *** $p < 0.001$, **** $p < 0.0001$
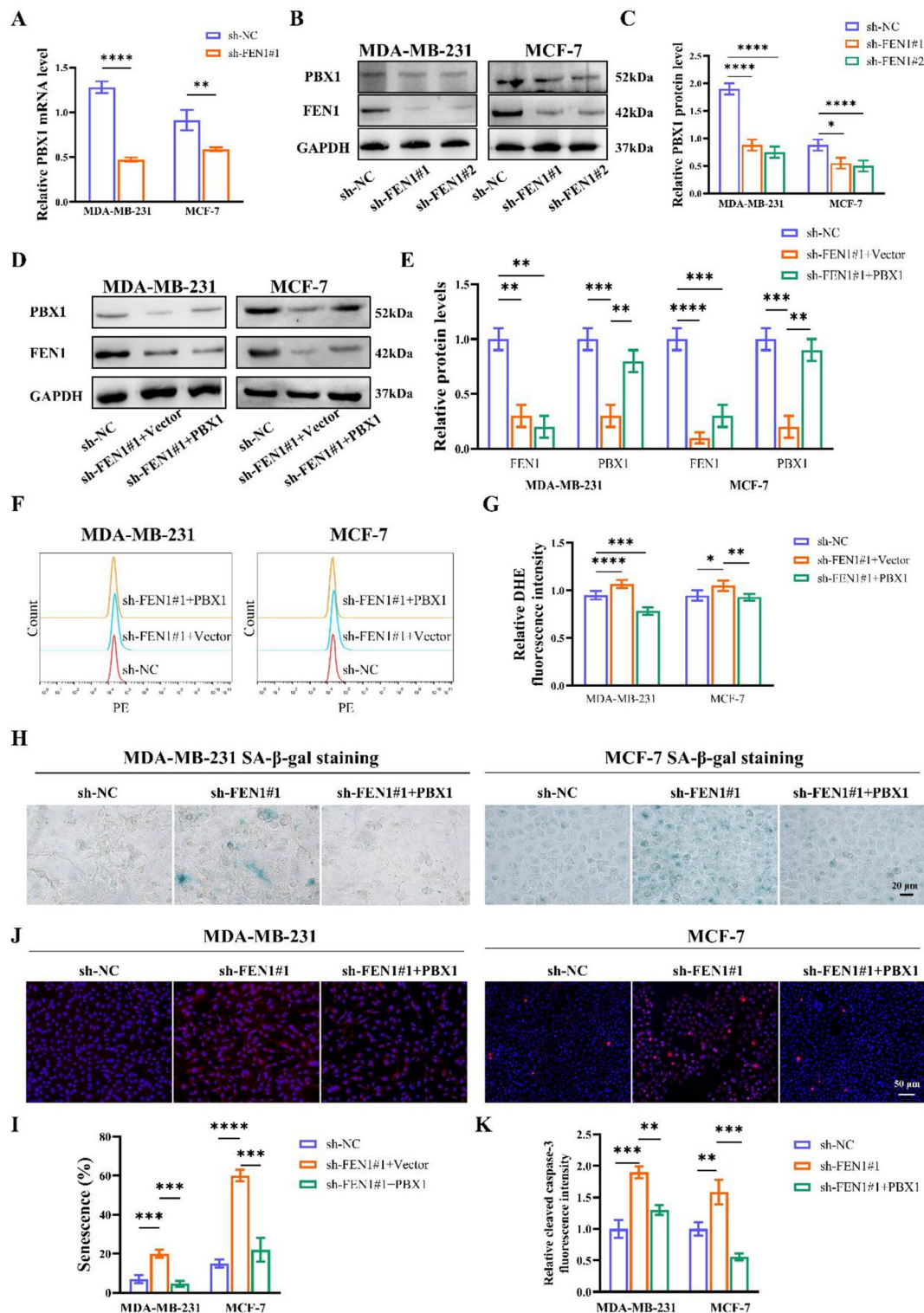
Fig. 5 PBX1 mediates the senescence and apoptosis of breast cancer cells induced by FEN1 inhibition. **A** The qRT-PCR and **B-C** Western blot analysis verified that PBX1 levels were decreased after FEN1 knockdown. **D-E** Western blot analysis showed the successful establishment of FEN1 knockdown cells with PBX1 overexpression (2.5 μg, 48 h). **F-G** ROS levels, **H-I** positive rates of SA-β-gal staining, as well as **J-K** the expression of cleaved caspase-3 were increased in FEN1 knockdown cells but decreased in FEN1 knockdown cells transfected with PBX1-expressing plasmids (1 μg, 48 h). Results are presented as mean ± SD from three independent experiments, * $p < 0.05$, ** $p < 0.01$, *** $p < 0.001$, **** $p < 0.0001$
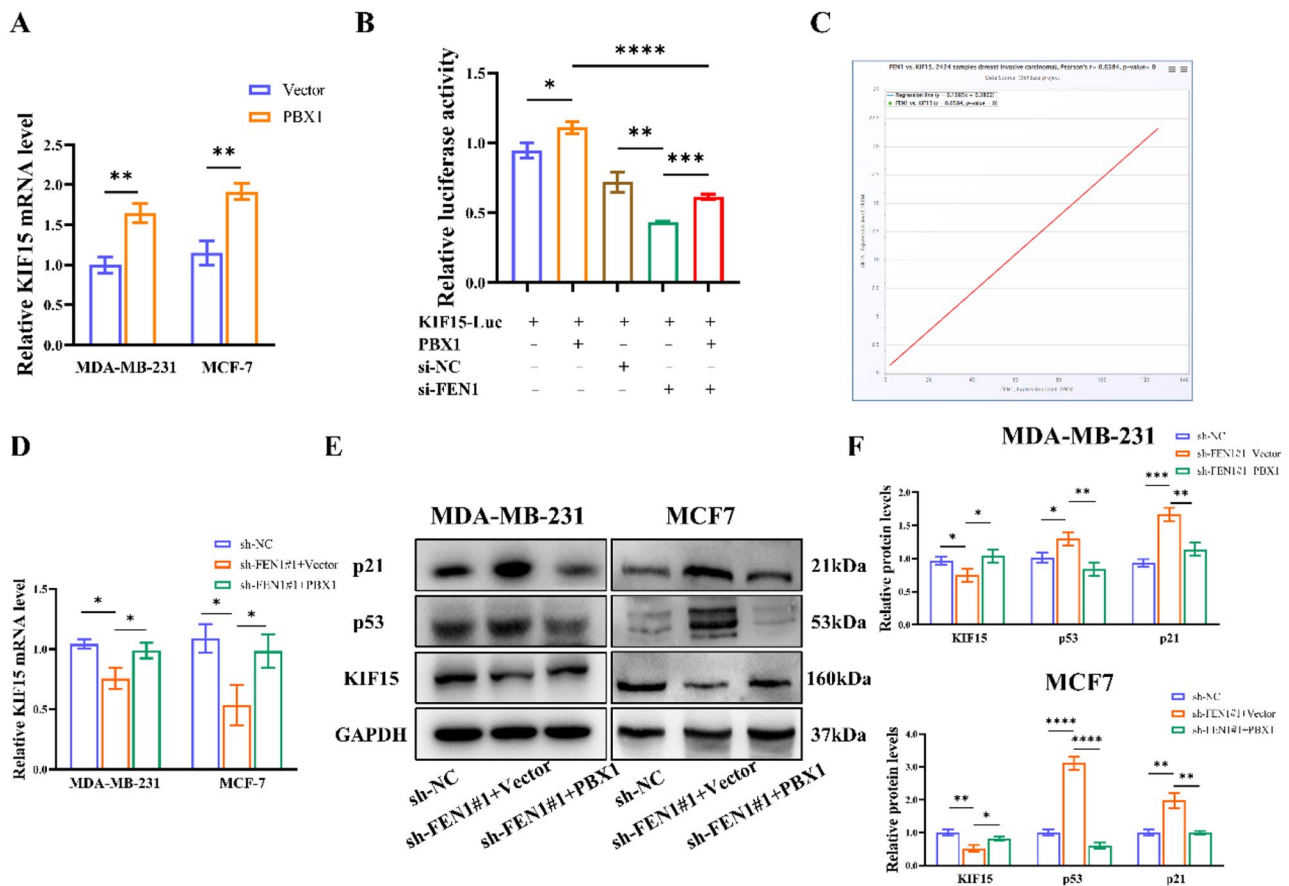
Fig. 6 FEN1 deficiency inhibits the transcription activity of PBX1. **A** The qRT-PCR analysis showed that KIF15 mRNA level was increased after PBX1 over-expression in breast cancer cells. **B** Luciferase assays confirmed that FEN1 downregulation decreased the transcription activity of PBX1 in HEK293T cells. **C** The correlation between FEN1 and KIF15 according to the ChIPBase v3.0 project. **D** The qRT-PCR and **E-F** Western blot analysis indicated that KIF15 levels were decreased in FEN1 knockdown cells while increased after cells transfected with PBX1-expressing plasmids (2.5 μg, 48 h). **E-F** Western blot analysis verified that p21 and p53 levels were increased in FEN1 knockdown cells while decreased after cells transfected with PBX1-expressing plasmids (2.5 μg, 48 h). Results are presented as mean ± SD from three independent experiments, * $p < 0.05$, ** $p < 0.01$, *** $p < 0.001$, **** $p < 0.0001$

FEN1 deficiency promotes breast cancer cell senescence and apoptosis in vivo

To verify the role of FEN1 in vivo, MDA-MB-231 cell lines (sh-NC and sh-FEN1#1) were selected to construct xenograft tumor models (4 in each group, a total of 8). Following a 6-week period of cell injection, each group of nude mice were sacrificed, and the tumors were collected and weighed. In comparison to the sh-NC group, the tumor volume and weight in the sh-FEN1#1 group were found to be smaller, as shown in Fig. 8A-C. In addition, the TGI value of sh-FEN1#1 group could reach 50.7%, indicating that FEN1 knockdown had a moderate therapeutic effect. The sh-FEN1#1 group exhibited significantly higher positive rates of DHE staining and SA-β-gal staining, as well as a higher percentage of apoptotic cells, compared to the sh-NC group (Fig. 8D-E). Furthermore, IHC analyses indicated that, compared to the sh-NC group, the expression of FEN1, Ki67, PBX1, and KIF15 was all reduced in the sh-FEN1#1 group (Fig. 8F-G). The in vivo experimental results demonstrated that

FEN1 knockdown downregulated PBX1 expression and promoted ROS levels as well as cell senescence and apoptosis in breast cancer cells, thereby inhibiting tumor growth. Collectively, these findings indicate that FEN1 interacts with PBX1, and its downregulation suppresses the expression and transcription activity of PBX1, thus enhancing intracellular ROS levels and then promoting senescence and apoptosis in breast cancer cells (Fig. 8H).

The expression of FEN1 is positively correlated with the expression of PBX1 in our local cohort

To investigate the relationship between FEN1 and PBX1 expression in breast cancer patients, we performed IHC analysis in collected paraffin sections from 50 patients with breast cancer and matched adjacent normal tissues. The expression levels of FEN1 and PBX1 were higher in cancer tissues compared with normal tissues (Fig. 9A-B). Notably, the expression level of FEN1 had a significant correlation with the expression of PBX1 in breast cancer ($r = 0.5987$, $p < 0.0001$) (Fig. 9C). Furthermore, breast
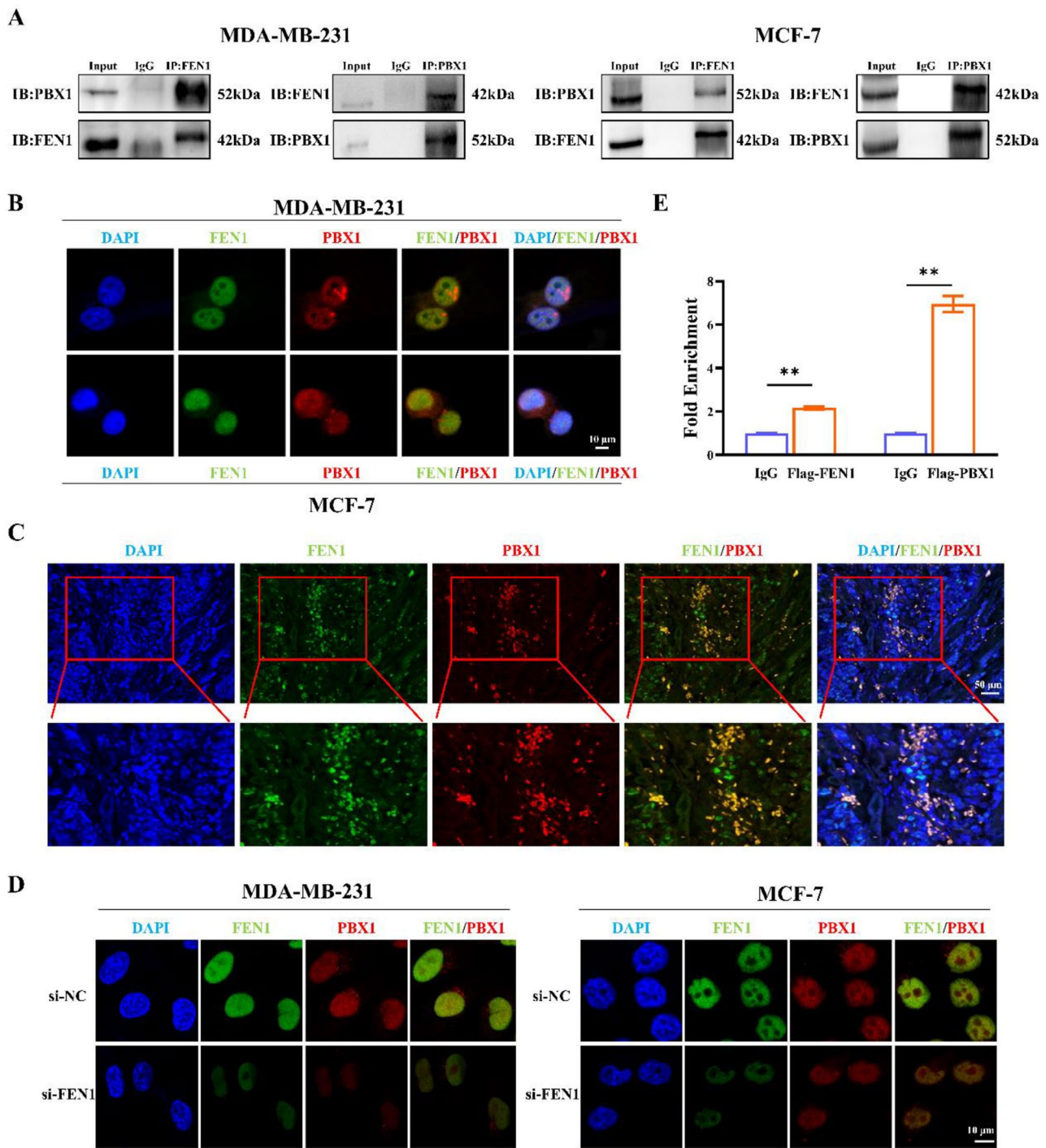
Fig. 7 FEN1 interacts with PBX1. **A** Co-IP analysis with anti-FEN1 or anti-PBX1 antibody in breast cancer cells. Immunostaining showed the colocalization of FEN1 and PBX1 in breast cancer cells (**B**) and tissues (**C**). **D** Immunostaining confirmed that FEN1 knockdown resulted in a significant reduction in the colocalization of FEN1 and PBX1 in breast cancer cells. **E** ChIP-qPCR analysis of FEN1 and PBX1 binding at the KIF15 promoter in HEK293T cells. Relative fold enrichments were shown. The value from control IgG ChIP-qPCR under the same condition was set as 1. Results are presented as mean ± SD from three independent experiments, ** $p < 0.01$

Wu *et al. Journal of Translational Medicine*   (2025) 23:248
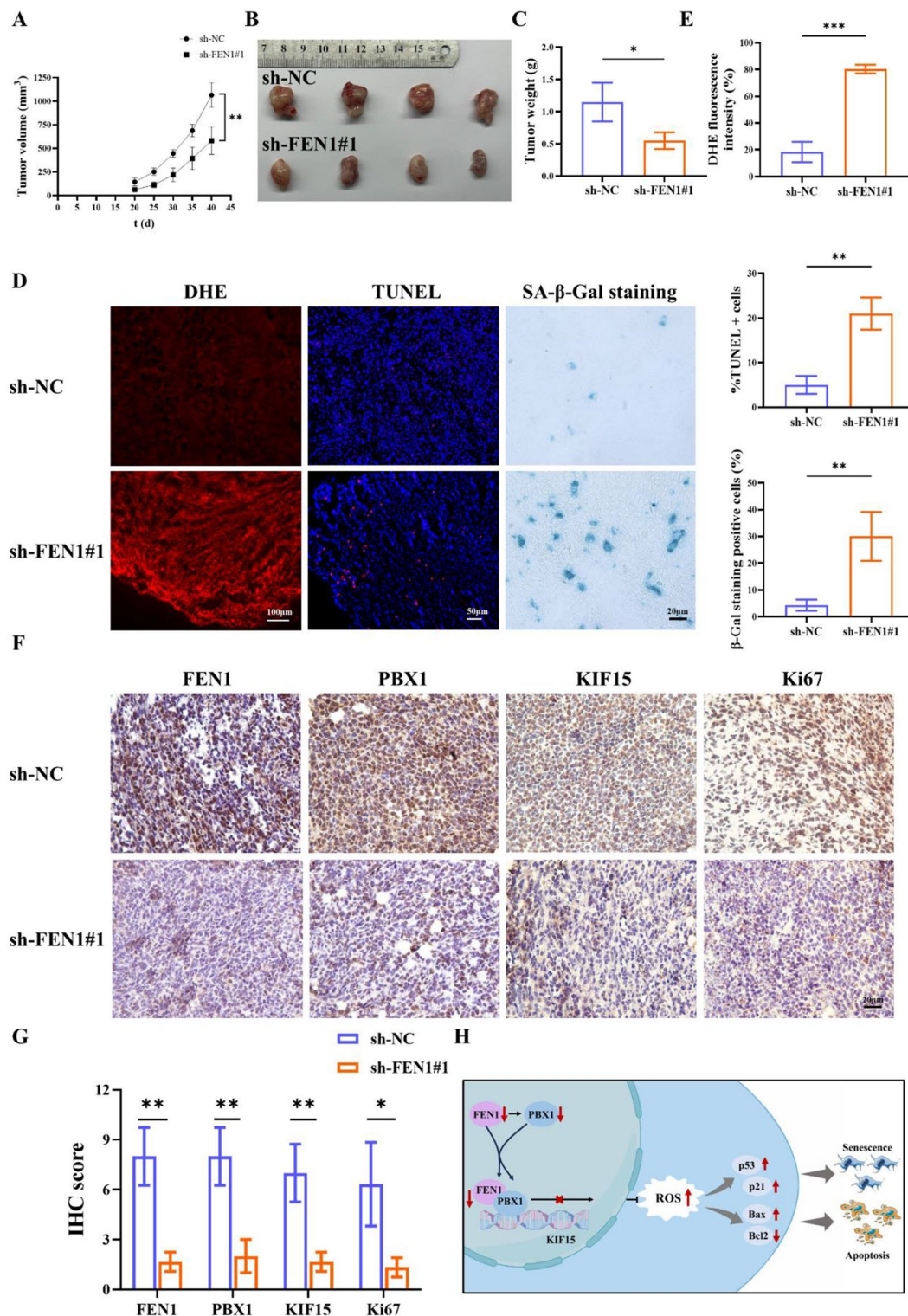
Page 15 of 20

Fig. 8 FEN1 deficiency promotes breast cancer cell senescence and apoptosis in vivo. **A** Tumor volume in the sh-NC and sh-FEN1#1 groups. **B** Tumors in sh-FEN1#1 group were notably smaller than those in sh-NC group. **C** Tumor weights in the sh-NC and sh-FEN1#1 groups. **D-E** DHE staining, TUNEL assay and SA-β-gal staining analysis indicated that the sh-FEN1#1 group had more positive cells than the sh-NC group (D, representative images; E, quantified results). **F-G** IHC was performed on the mouse tumor tissues to evaluate the expressions of FEN1, PBX1, KIF15 and Ki67 (**F**, representative images; **G**, IHC score of FEN1, PBX1, KIF15 and Ki67). **H** Proposed model: knockdown of FEN1 facilitates breast cancer cell senescence and apoptosis by downregulating the expression and transcription activity of PBX1 and then increasing intracellular ROS levels. $n = 4$, * $p < 0.05$, ** $p < 0.01$, *** $p < 0.001$
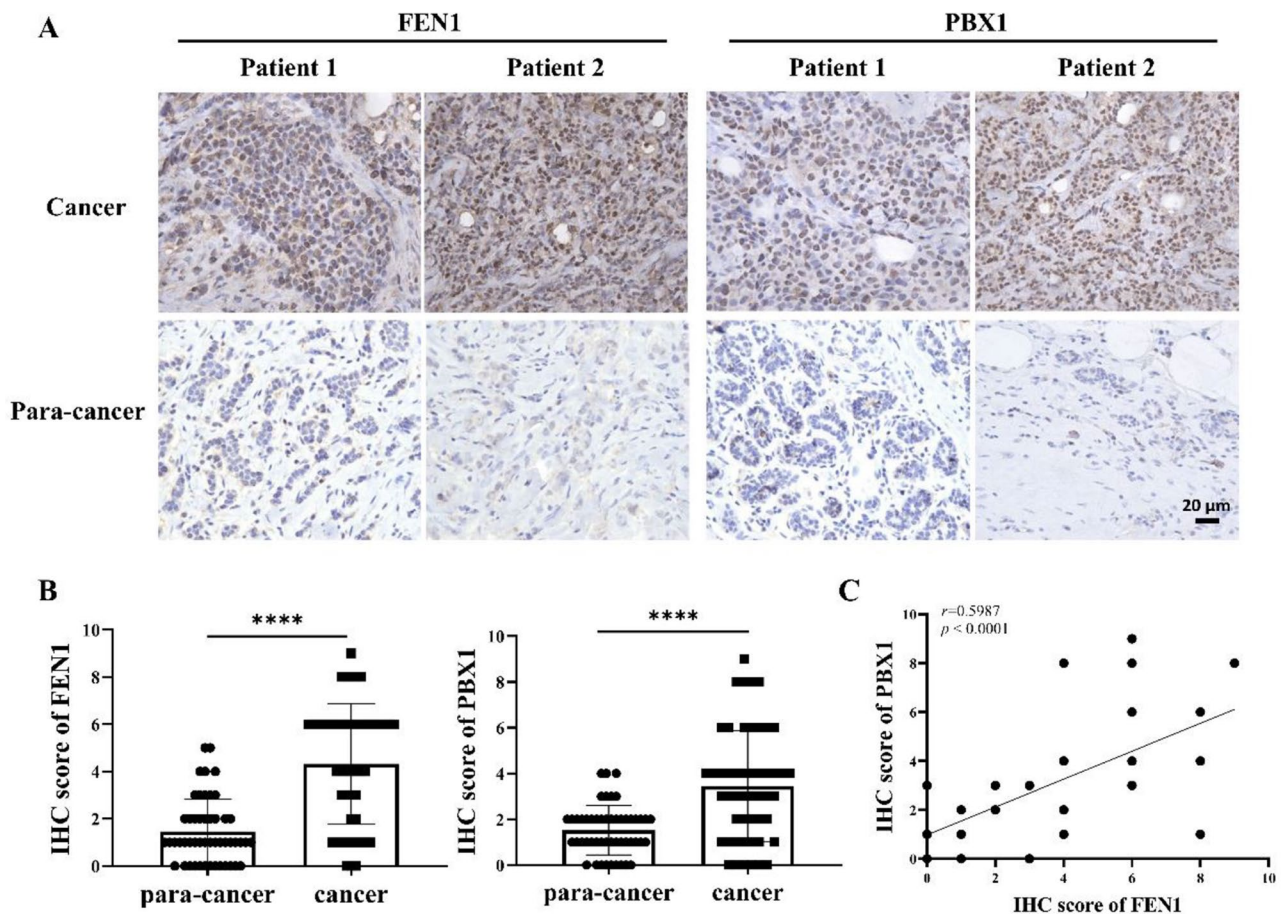
Fig. 9 The expression of FEN1 is positively correlated with the expression of PBX1 in our local cohort. **A** IHC analysis of FEN1 and PBX1 were performed in breast cancer tissues and adjacent tissues. **B** IHC scores of FEN1 and PBX1 were calculated. **C** Correlation and simple linear regression of FEN1 and PBX1 in breast cancer tissues. $n = 50$, **** $p < 0.0001$

cancer patients with large tumor size (≥ 2 cm), lymph node metastasis or late TNM stage (stage III-IV), had higher levels of FEN1 (Supplementary Table 1). In contrast, higher expression of PBX1 was only associated with late tumor stage (Supplementary Table 1). These results suggest that FEN1 expression is positively correlated with PBX1 expression in breast cancer patients.

Discussion

Senescence induction (pro-senescence therapy) is being actively investigated for cancer treatment [39]. This study aims to explore the relationship between FEN1 and breast cancer cells senescence. Initially, we observed that overexpressing FEN1 stimulated breast cancer cell proliferation, while its knockdown suppressed it, aligning with previous reports [21, 40]. Additionally, apart from the common G1 phase arrest [41], FEN1 downregulation led to breast cancer cell arrest in the S phase. Consistent with our study, CXXC zinc finger protein 1 downregulation promotes ovarian cancer cell senescence by inducing S-phase arrest [42]. In this study, FEN1 negatively

regulated cancer cell apoptosis and senescence, thereby inhibiting cell growth. Aligning with our findings, numerous studies on FEN1 and tumor cell apoptosis revealed moderate increases in apoptotic rates from FEN1 downregulation alone [26, 43, 44]. Not surprisingly, both genetic and pharmacologic inhibition of FEN1 usually requires the combination of anticancer drugs to exert the pro-apoptotic effect [26, 43, 44]. To date, there have been no reports indicating that downregulation of FEN1 can promote cancer cellular senescence. Based on our research, FEN1-targeted pro-senescence cancer therapy might be a potential treatment option. Notably, the apoptotic resistance of cellular senescence is that senescent cells themselves are not susceptible to apoptosis. Whether senescent cells affect the apoptosis of other non-senescent cells is uncertain, for the following reasons:1) FEN1 knockdown itself has an effect on cell apoptosis; 2) SASP factors secreted by senescent cells may affect the apoptosis of other cells. In our study, SASP factors secreted by senescent cells could inhibit the proliferation of other cells and promote their senescence.

Elevated intracellular ROS level is a significant factor contributing to cell apoptosis and senescence [30]. The simultaneous application of FEN1 knockdown and arsenic trioxide (ATO) enhances the levels of ROS in breast cancer cells by reducing the nuclear translocation of nuclear factor erythroid 2-related factor 2 (Nrf2) [43]. Our findings reveal that FEN1 overexpression lowers ROS levels in breast cancer cells, whereas FEN1 knockdown increases them. Moreover, FEN1 knockdown promotes breast cancer cell senescence and apoptosis by elevating ROS levels. Consistently, FEN1 knockdown also enhanced ROS levels, cell senescence, and apoptosis in tumor-bearing nude mice.

Next, transcriptome sequencing and bioinformatics analysis affirmed FEN1's association with cell senescence, corroborating earlier bioinformatics research [27]. Analysis of differentially expressed genes showed FEN1 knockdown boosted SASP factors expression, echoing findings that FEN1 inhibitor SC13 increases chemokines secretion in tumor cells, enhancing CAR-T cell infiltration [45]. It is noteworthy that the increase in SASP factors in MDA-MB-231 cells due to FEN1 knockdown was greater in magnitude than the elevation observed in MCF-7 cells. Moreover, the variety of SASP factors affected by FEN1 downregulation was also broader in MDA-MB-231 cells compared to MCF-7 cells. These differences in outcomes may be related to the inherent genetic differences between the two cell lines. In addition, we have demonstrated that SASP factors secreted by FEN1 knockdown cells inhibited tumor cell proliferation in vitro. Given that FEN1 has an immunoregulatory role [25, 26] and its association with the SASP secretion in cancer cells, the crosstalk between FEN1 knockdown tumor cells and immune cells within the tumor microenvironment warrants further investigation. Based on previous studies and our sequencing data, the homeodomain transcription factor PBX1 [17] is a potential target of FEN1. PBX1 plays a key role in the development of various organs like bone, lung, heart, and kidney [46], and is significantly upregulated in various cancers, including esophageal, breast, melanoma, and prostate cancers [17]. Our study supports these findings, as we noted strong PBX1 expression in breast cancer tissues, significantly correlating with worse prognosis. Moreover, PBX1 significantly influences ROS production, cell apoptosis, and cell senescence. Li et al. reported that PBX1 overexpression inhibited 6-hydroxydopamine -induced intracellular ROS production in human neuroblastoma cells [47]. PBX1 overexpression restrains apoptosis and senescence of human hair follicle mesenchymal stem cells by reducing ROS levels [48, 49]. Our study confirmed the inhibitory impact of PBX1 on the production of ROS and cell apoptosis. However, there is currently no available study that investigates the relationship between PBX1 and tumor cell senescence. In this

study, we found that PBX1 inhibited the senescence of breast cancer cells. Although PBX1 was not directly correlated with immune response pathways in cancer, PBX1 has transcriptional targets related to immune system. For instance, PBX1 is involved in the transcriptional activation of the anti-inflammatory cytokines IL10 and CD46 [50, 51]. Therefore, the FEN1-PBX1 axis warrants further investigation within the realm of cancer immunology.

Finally, we explored whether FEN1 regulates breast cancer cell senescence and apoptosis through PBX1. Our results showed that the down-regulation of FEN1 caused the elevated cell senescence and apoptosis mainly by down-regulating PBX expression. In our local breast cancer cohort, we found that the expression of FEN1 or PBX1 in cancer tissues was higher than that in adjacent non-cancerous tissues. Furthermore, a positive correlation was identified between the expression levels of FEN1 and PBX1 in the cohort. PBX1 is known to be a transcription factor and KIF15 is one of the target genes of PBX1 [34]. KIF15 is overexpressed in multiple cancers, correlating with poor prognosis [52]. Moreover, KIF15 curbs ROS generation in gastric and liver cancer cells, thus dampening cell apoptosis and senescence [53, 54]. The dual-luciferase reporter assay confirmed that PBX1 overexpression only partly restored the transcription of KIF15 promoter, and FEN1 knockdown significantly reduced it, suggesting multiple ways FEN1 might influence PBX1's transcription activity. It has been reported that some proteins can interact with downstream transcription factors and regulate their transcription activities [37, 38]. In the present study, it was found that FEN1 interacts with PBX1 and co-localizes with PBX1 in the nucleus of breast cancer cells. Downregulation of FEN1 results in a decrease in its colocalization with PBX1. Further investigation is required to elucidate whether and how their interaction influences transcription activity. Collectively, these findings indicate that FEN1 interacts with PBX1, and that downregulation of FEN1 suppresses both the expression and transcription activity of PBX1.

Indeed, FEN1 knockdown caused only moderate tumor cell senescence and apoptosis, and tumor growth inhibition in vivo. Possible reasons include: 1) cell fate is affected by many factors, and only knocking down FEN1 expression cannot completely inhibit tumor cell growth; 2) senescent cells induced by FEN1 knockdown could secret some SASP factors, which may offset some of the anti-tumor effect of sh-FEN1. Even though we demonstrated that SASP factors secreted by FEN1 knockdown cells could inhibit tumor cell proliferation in vitro, but, the types and functions of SASP factors secreted by early and late senescent tumor cells are different [33]. SASP factors secreted by senescent tumor cells in the late stage even enhance the malignant potential of tumor cells [33]. Based on the heterogeneous effects of cellular senescence

on tumor cells, scholars have proposed a variety of cancer treatment strategies. It is worth noting that pro-senescence therapy is often combined with senolytics therapy (to eliminate senescent tumor cells by inducing apoptosis of senescent cells) for the treatment of cancer [55, 56], known as 'one-two punch' sequential cancer therapy. Therefore, combining FEN1 knockdown with senolytics therapy is a potential strategy for cancer treatment.

Conclusions

This study represents the first identification of the relationship between FEN1 and cellular senescence in breast cancer, and elucidates the specific mechanism by which FEN1 regulates breast cancer cell senescence. Knockdown of FEN1 facilitates breast cancer cell senescence by downregulating the expression and transcription activity of PBX1 and then increasing intracellular ROS levels. This study contributes to the functional research of FEN1 in tumors, and offers evidence supporting the pro-senescence therapy. Based on the 'one-two punch' sequential cancer therapy, it is of great potential to combine senolytics with targeting FEN1 to exert better anti-tumor effect.

Abbreviations

SA-β-gal	Senescence-Associated β-galactosidase
SASP	Senescence-Associated Secretory Phenotype
ERK5	Extracellular signal-Regulated Kinase 5
NIPSNAP1	Non-neuronal SNAP25-like protein homologue 1
RPIA	Ribose-5-Phosphate Isomerase A
ROS	Reactive Oxygen Species
AQP8	Aquaporin 8
PTEN	Phosphatase and Tensin Homologue
AKT	Serine/threonine protein kinase
WWOX	WW domain-containing Oxidoreductase
SIRT3	Sirtuin 3
SOD2	Superoxide Dismutase 2
FEN1	Flap Endonuclease 1
PBX1	Pre-B-cell leukemia homeobox transcription factor 1
KEGG	Kyoto Encyclopedia of Genes and Genomes
TIMER2.0	Tumor Immune Estimation Resource, version 2
GEPIA2	Gene Expression Profiling Interactive Analysis, version 2
KIF15	Kinesin Family member 15
qRT-PCR	Quantitative Real-Time Polymerase Chain Reaction
CCK-8	Cell Counting kit-8
DHE	Dihydroethidium
Co-IP	Co-Immunoprecipitation
ChIP-qPCR	Chromatin Immunoprecipitation -quantitative Polymerase Chain Reaction
IHC	Immunohistochemistry
TUNEL	Terminal Deoxynucleotidyl Transferase dUTP Nick End Labeling
NAC	N-Acetylcysteine
NOX2/4	NADPH Oxidase 2/4
2-ME2	2-Methoxyestradiol
CFP1	CXXC zinc Finger Protein 1
ATO	Arsenic Trioxide
Nrf2	Nuclear Factor Erythroid 2-related factor 2

Supplementary Information

The online version contains supplementary material available at https://doi.org/10.1186/s12967-025-06216-9.

Supplementary File(including supplementary Figures 1-8 and Tables 1-3)

Declarations

Ethical approval
All the patients, diagnosed and treated at Jiangsu Cancer Hospital, provided written informed consents. The whole study conformed to the Helsinki Declaration. The study protocol was approved by the Ethical Committee of Jiangsu Cancer Hospital. All methods involving animals in this study were performed in accordance with the institutional ethical guidelines on animal care and were approved by the Ethics Committee of the Medical College of Yangzhou University.

Consent for publication
Not applicable.

Conflict of interest
The authors declare no potential conflicts of interest.

Author details
[1]Institute of Translational Medicine, Medical College, Yangzhou University, Yangzhou 225009, China
[2]Jiangsu Key Laboratory of Integrated Traditional Chinese and Western Medicine for Prevention and Treatment of Senile Diseases, Yangzhou University, Yangzhou 225009, China
[3]Department of Pathology, Jiangsu Cancer Hospital, Nanjing 210018, China

References
1. Siegel RL, Giaquinto AN, Jemal A. Cancer statistics, 2024. CA Cancer J Clin. 2024;74(1):12–49.
2. Cardoso MJ, Poortmans P, Senkus E, Gentilini OD, Houssami N. Breast cancer highlights from 2023: knowledge to guide practice and future research. Breast. 2024;74:103674.
3. Freitas AJA, Causin RL, Varuzza MB, Calfa S, Hidalgo Filho CMT, Komoto TT, Souza CP, Marques MMC. Liquid Biopsy as a Tool for the diagnosis, treatment, and monitoring of breast Cancer. Int J Mol Sci 2022, 23(17).
4. Mohamad Kamal NS, Safuan S, Shamsuddin S, Foroozandeh P. Aging of the cells: insight into cellular senescence and detection methods. Eur J Cell Biol. 2020;99(6):151108.
5. Schmitt CA, Wang B, Demaria M. Senescence and cancer - role and therapeutic opportunities. Nat Rev Clin Oncol. 2022;19(10):619–36.
6. Tubita A, Lombardi Z, Tusa I, Lazzeretti A, Sgrignani G, Papini D, Menconi A, Gagliardi S, Lulli M, Dello Sbarba P, et al. Inhibition of ERK5 elicits Cellular Senescence in Melanoma via the cyclin-dependent kinase inhibitor p21. Cancer Res. 2022;82(3):447–57.

7.   Gao E, Sun X, Thorne RF, Zhang XD, Li J, Shao F, Ma J, Wu M. NIPSNAP1 directs dual mechanisms to restrain senescence in cancer cells. J Transl Med. 2023;21(1):401.
8.   Nieh YC, Chou YT, Chou YT, Wang CY, Lin SX, Ciou SC, Yuh CH, Wang HD. Suppression of Ribose-5-Phosphate Isomerase a induces ROS to Activate Autophagy, apoptosis, and Cellular Senescence in Lung Cancer. Int J Mol Sci 2022, 23(14).
9.   Wang L, Lankhorst L, Bernards R. Exploiting senescence for the treatment of cancer. Nat Rev Cancer. 2022;22(6):340–55.
10. Hao Z, Huajun S, Zhen G, Yu X, Qian L, Ziling C, Zihao S, Qingqian X, Shujuan Z. AQP8 promotes glioma proliferation and growth, possibly through the ROS/PTEN/AKT signaling pathway. BMC Cancer. 2023;23(1):516.
11. Liu CW, Chen PH, Yu TJ, Lin KJ, Chang LC. WWOX modulates ROS-Dependent senescence in bladder Cancer. Molecules 2022, 27(21).
12. Davalli P, Mitic T, Caporali A, Lauriola A, D'Arca D. ROS, Cell Senescence, and Novel Molecular Mechanisms in Aging and Age-Related Diseases. *Oxid Med Cell Longev* 2016, 2016:3565127.
13. Kao TW, Chen HH, Lin J, Wang TL, Shen YA. PBX1 as a novel master regulator in cancer: its regulation, molecular biology, and therapeutic applications. Biochim Biophys Acta Rev Cancer. 2024;1879(2):189085.
14. Park JT, Shih Ie M, Wang TL. Identification of Pbx1, a potential oncogene, as a Notch3 target gene in ovarian cancer. Cancer Res. 2008;68(21):8852–60.
15. Zhang LX, Xu L, Zhang CH, Lu YH, Ji TH, Ling LJ. uc.38 induces breast cancer cell apoptosis via PBX1. Am J Cancer Res. 2017;7(12):2438–51.
16. Yanagi H, Watanabe T, Nishimura T, Hayashi T, Kono S, Tsuchida H, Hirata M, Kijima Y, Takao S, Okada S, et al. Upregulation of S100A10 in metastasized breast cancer stem cells. Cancer Sci. 2020;111(12):4359–70.
17. Shen YA, Jung J, Shimberg GD, Hsu FC, Rahmanto YS, Gaillard SL, Hong J, Bosch J, Shih IM, Chuang CM, et al. Development of small molecule inhibitors targeting PBX1 transcription signaling as a novel cancer therapeutic strategy. iScience. 2021;24(11):103297.
18. Zheng L, Jia J, Finger LD, Guo Z, Zer C, Shen B. Functional regulation of FEN1 nuclease and its link to cancer. Nucleic Acids Res. 2011;39(3):781–94.
19. Zhang K, Keymeulen S, Nelson R, Tong TR, Yuan YC, Yun X, Liu Z, Lopez J, Raz DJ, Kim JY. Overexpression of Flap Endonuclease 1 correlates with enhanced proliferation and poor prognosis of Non-small-cell Lung Cancer. Am J Pathol. 2018;188(1):242–51.
20. Abdel-Fatah TM, Russell R, Albarakati N, Maloney DJ, Dorjsuren D, Rueda OM, Moseley P, Mohan V, Sun H, Abbotts R, et al. Genomic and protein expression analysis reveals flap endonuclease 1 (FEN1) as a key biomarker in breast and ovarian cancer. Mol Oncol. 2014;8(7):1326–38.
21. Zeng X, Qu X, Zhao C, Xu L, Hou K, Liu Y, Zhang N, Feng J, Shi S, Zhang L, et al. FEN1 mediates miR-200a methylation and promotes breast cancer cell growth via MET and EGFR signaling. Faseb j. 2019;33(10):10717–30.
22. Bian S, Ni W, Zhu M, Zhang X, Qiang Y, Zhang J, Ni Z, Shen Y, Qiu S, Song Q, et al. Flap endonuclease 1 facilitated Hepatocellular Carcinoma Progression by enhancing USP7/MDM2-mediated P53 inactivation. Int J Biol Sci. 2022;18(3):1022–38.
23. Yuwei X, Bingzi D, Zhaowei S, Yujie F, Wei Z, Kun L, Kui L, Jingyu C, Chengzhan Z. FEN1 promotes cancer progression of cholangiocarcinoma by regulating the Wnt/β-catenin signaling pathway. Dig Liver Dis. 2024;56(4):695–704.
24. Wu M, Huang X, Wu B, Zhu M, Zhu Y, Yu L, Lan T, Liu J. The endonuclease FEN1 mediates activation of STAT3 and facilitates proliferation and metastasis in breast cancer. Mol Biol Rep. 2024;51(1):553.
25. Wang S, Wang X, Sun J, Yang J, Wu D, Wu F, Zhou H. Down-regulation of DNA key protein-FEN1 inhibits OSCC growth by affecting immunosuppressive phenotypes via IFN-γ/JAK/STAT-1. Int J Oral Sci. 2023;15(1):17.
26. Wang X, Xu S, Fu T, Wu Y, Sun W. Combination of downregulating FEN1 and PD-1 blockade enhances antitumor activity of CD8 + T cells against HNSCC cells in vitro. J Oral Pathol Med. 2023;52(9):834–42.
27. Shen X, Wang M, Chen W, Xu Y, Zhou Q, Zhu T, Wang G, Cai S, Han Y, Xu C, et al. Senescence-related genes define prognosis, immune contexture, and pharmacological response in gastric cancer. Aging. 2023;15(8):2891–905.
28. Amin MB, Greene FL, Edge SB, Compton CC, Gershenwald JE, Brookland RK, Meyer L, Gress DM, Byrd DR, Winchester DP. The Eighth Edition AJCC Cancer staging Manual: continuing to build a bridge from a population-based to a more personalized approach to cancer staging. CA Cancer J Clin. 2017;67(2):93–9.
29. Armartmuntree N, Murata M, Techasen A, Yongvanit P, Loilome W, Namwat N, Pairojkul C, Sakonsinsiri C, Pinlaor S, Thanan R. Prolonged oxidative stress down-regulates early B cell factor 1 with inhibition of its tumor suppressive function against cholangiocarcinoma genesis. Redox Biol. 2018;14:637–44.
30. Wang Y, Qi H, Liu Y, Duan C, Liu X, Xia T, Chen D, Piao HL, Liu HX. The double-edged roles of ROS in cancer prevention and therapy. Theranostics. 2021;11(10):4839–57.
31. Fukai T, Ushio-Fukai M. Cross-talk between NADPH oxidase and Mitochondria: role in ROS Signaling and Angiogenesis. Cells 2020, 9(8).
32. Saadi A, Sandouka S, Grad E, Singh PK, Shekh-Ahmad T. Spatial, temporal, and cell-type-specific expression of NADPH oxidase isoforms following seizure models in rats. Free Radic Biol Med. 2022;190:158–68.
33. Acosta JC, Banito A, Wuestefeld T, Georgilis A, Janich P, Morton JP, Athineos D, Kang TW, Lasitschka F, Andrulis M, et al. A complex secretory program orchestrated by the inflammasome controls paracrine senescence. Nat Cell Biol. 2013;15(8):978–90.
34. Liu Y, Zhai E, Chen J, Qian Y, Zhao R, Ma Y, Liu J, Huang Z, Cai S, Chen J. M(6) A-mediated regulation of PBX1-GCH1 axis promotes gastric cancer proliferation and metastasis by elevating tetrahydrobiopterin levels. Cancer Commun (Lond). 2022;42(4):327–44.
35. Tao J, Sun G, Li Q, Zhi X, Li Z, He Z, Chen H, Zhou A, Ye J, Xu G, et al. KIF15 promotes the evolution of gastric cancer cells through inhibition of reactive oxygen species-mediated apoptosis. J Cell Physiol. 2020;235(12):9388–98.
36. Li Q, Qiu J, Yang H, Sun G, Hu Y, Zhu D, Deng Z, Wang X, Tang J, Jiang R. Kinesin family member 15 promotes cancer stem cell phenotype and malignancy via reactive oxygen species imbalance in hepatocellular carcinoma. Cancer Lett. 2020;482:112–25.
37. Hou Z, Guo K, Sun X, Hu F, Chen Q, Luo X, Wang G, Hu J, Sun L. TRIB2 functions as novel oncogene in colorectal cancer by blocking cellular senescence through AP4/p21 signaling. Mol Cancer. 2018;17(1):172.
38. Sun Y, Lin P, Zhou X, Ren Y, He Y, Liang J, Zhu Z, Xu X, Mao X. TRIM26 promotes non-small cell lung cancer survival by inducing PBX1 degradation. Int J Biol Sci. 2023;19(9):2803–16.
39. Birch J, Gil J. Senescence and the SASP: many therapeutic avenues. Genes Dev. 2020;34(23–24):1565–76.
40. Xu L, Shen JM, Qu JL, Song N, Che XF, Hou KZ, Shi J, Zhao L, Shi S, Liu YP, et al. FEN1 is a prognostic biomarker for ER + breast cancer and associated with tamoxifen resistance through the ERα/cyclin D1/Rb axis. Ann Transl Med. 2021;9(3):258.
41. Sun Z, Pan X, Zou Z, Ding Q, Wu G, Peng G. Increased SHP-1 expression results in radioresistance, inhibition of cellular senescence, and cell cycle redistribution in nasopharyngeal carcinoma cells. Radiat Oncol. 2015;10:152.
42. Yang LQ, Hu HY, Han Y, Tang ZY, Gao J, Zhou QY, Liu YX, Chen HS, Xu TN, Ao L, et al. CpG-binding protein CFP1 promotes ovarian cancer cell proliferation by regulating BST2 transcription. Cancer Gene Ther. 2022;29(12):1895–907.
43. Xin X, Wen T, Gong LB, Deng MM, Hou KZ, Xu L, Shi S, Qu XJ, Liu YP, Che XF, et al. Inhibition of FEN1 increases Arsenic Trioxide-Induced ROS Accumulation and Cell Death: Novel Therapeutic potential for Triple negative breast Cancer. Front Oncol. 2020;10:425.
44. Wang Z, Yong C, Fu Y, Sun Y, Guo Z, Liu SB, Hu Z. Inhibition of FEN1 promotes DNA damage and enhances chemotherapeutic response in prostate cancer cells. Med Oncol. 2023;40(8):242.
45. Dong Y, Wang Y, Yin X, Zhu H, Liu L, Zhang M, Chen J, Wang A, Huang T, Hu J, et al. FEN1 inhibitor SC13 promotes CAR-T cells infiltration into solid tumours through cGAS-STING signalling pathway. Immunology. 2023;170(3):388–400.
46. Welsh IC, Hart J, Brown JM, Hansen K, Rocha Marques M, Aho RJ, Grishina I, Hurtado R, Herzlinger D, Ferretti E, et al. Pbx loss in cranial neural crest, unlike in epithelium, results in cleft palate only and a broader midface. J Anat. 2018;233(2):222–42.
47. Li B, An D, Zhu S. PBX1 attenuates 6-OHDA-induced oxidative stress and apoptosis and affects PINK1/PARKIN expression in dopaminergic neurons via FOXA1. Cytotechnology. 2022;74(2):217–29.
48. Wang Y, Sui Y, Niu Y, Liu D, Xu Q, Liu F, Zuo K, Liu M, Sun W, Wang Z, et al. PBX1-SIRT1 positive feedback Loop attenuates ROS-Mediated HF-MSC senescence and apoptosis. Stem Cell Rev Rep. 2023;19(2):443–54.
49. Wang Y, Sui Y, Lian A, Han X, Liu F, Zuo K, Liu M, Sun W, Wang Z, Liu Z, et al. PBX1 attenuates hair follicle-derived mesenchymal stem cell senescence and apoptosis by alleviating reactive oxygen species-mediated DNA damage instead of enhancing DNA damage repair. Front Cell Dev Biol. 2021;9:739868.
50. Chung EY, Liu J, Homma Y, Zhang Y, Brendolan A, Saggese M, Han J, Silverstein R, Selleri L, Ma X. Interleukin-10 expression in macrophages during phagocytosis of apoptotic cells is mediated by homeodomain proteins Pbx1 and Prep-1. *Immunity* 2007, 27(6):952–964.
51. Thiaville MM, Stoeck A, Chen L, Wu RC, Magnani L, Oidtman J, Shih Ie M, Lupien M, Wang TL. Identification of PBX1 target genes in cancer cells by global mapping of PBX1 binding sites. PLoS ONE. 2012;7(5):e36054.

52. Mi J, Ma S, Chen W, Kang M, Xu M, Liu C, Li B, Wu F, Liu F, Zhang Y, et al. Integrative Pan-cancer analysis of KIF15 reveals its diagnosis and prognosis value in nasopharyngeal carcinoma. Front Oncol. 2022;12:772816.

53. Cerella C, Grandjenette C, Dicato M, Diederich M. Roles of apoptosis and Cellular Senescence in Cancer and Aging. Curr Drug Targets. 2016;17(4):405–15.

54. Jung SH, Lee M, Park HA, Lee HC, Kang D, Hwang HJ, Park C, Yu DM, Jung YR, Hong MN, et al. Integrin α6β4-Src-AKT signaling induces cellular senescence by counteracting apoptosis in irradiated tumor cells and tissues. Cell Death Differ. 2019;26(2):245–59.

55. Kirkland JL, Tchkonia T. Senolytic drugs: from discovery to translation. J Intern Med. 2020;288(5):518–36.

56. Zhang Y, Xiao B, Yuan S, Ding L, Pan Y, Jiang Y, Sun S, Ke X, Cai L, Jia L. Tryptanthrin targets GSTP1 to induce senescence and increases the susceptibility to apoptosis by senolytics in liver cancer cells. Redox Biol. 2024;76:103323.